

Excitation of negative energy surface magnetohydrodynamic waves in an incompressible cylindrical plasma

D. J. YU^{1,2} AND V. M. NAKARIAKOV^{2,3}

¹*Department of Astronomy and Space Science, Kyung Hee University, 1732, Deogyong-daero, Yongin, Gyeonggi 17104, South Korea*

²*School of Space Research, Kyung Hee University, 1732, Deogyong-daero, Yongin, Gyeonggi 17104, South Korea*

³*St. Petersburg Branch, Special Astrophysical Observatory, Russian Academy of Sciences, 196140, St. Petersburg, Russia*

(Received; Revised; Accepted)

Submitted to ApJ

ABSTRACT

Negative energy wave phenomena may appear in shear flows in the presence of a wave decay mechanism and external energy supply. We study the appearance of negative energy surface waves in a plasma cylinder in the incompressible limit. The cylinder is surrounded by an axial magnetic field and by a plasma of different density. Considering flow inside and viscosity outside the flux tube, we derive dispersion relations, and obtain analytical solutions for the phase speed and growth rate (increment) of the waves. It is found that the critical speed shear for the occurrence of the dissipative instability associated with negative energy waves (NEWs) and the threshold of Kelvin–Helmholtz instability (KHI) depend on the axial wavelength. The critical shear for the appearance of sausage NEW is lowest for the longest axial wavelengths, while for kink waves the minimum value of the critical shear is reached for the axial wavelength comparable to the diameter of the cylinder. The range between the critical speed of the dissipative instability and the KHI threshold is shown to depend on the difference of the Alfvén speeds inside and outside of the cylinder. For all axial wavenumbers, NEW appears for the shear flow speeds lower than the KHI threshold. It is easier to excite NEW in an underdense cylinder than in an overdense one. The negative energy surface waves can be effectively generated for azimuthal number $m = 0$ with a large axial wave number and for higher modes ($m > 0$) with a small axial wave number.

Keywords: magnetohydrodynamics(MHD) – waves – Sun: oscillations – Sun: atmosphere

1. INTRODUCTION

The solar atmosphere is a highly structured and dynamic medium with pronounced non-uniformities of the macroscopic parameters of the plasma, such as the density and temperature, and the magnetic field, and also with a number of transient and long-living plasma flows. The non-uniform nature of the atmosphere strongly affects the propagation of magnetohydrodynamic (MHD) waves, leading to the appearance of the wave dispersion, enhanced damping, mode coupling, amplification and many other effects (e.g., Edwin, & Roberts 1983; Ruderman & Roberts 2002; De Moortel & Nakari-

akov 2012; Jess & Verth 2016; Verth & Jess 2016; Goossens et al. 2019, and references therein). In particular, shear flows may greatly modify magnetohydrodynamic (MHD) wave propagation (e.g., Goossens et al. 1992; Nakariakov, & Roberts 1995). Strong shear can induce Kelvin–Helmholtz instability (KHI) (Chandrasekhar 1961; Zaqarashvili et al. 2015). In addition, the effect of overreflection may occur for MHD waves reflected from a plasma non-uniformity with a velocity shear (Fejer 1963; Sen 1963; McKenzie 1970; Nakaryakov & Stepanyants 1994; Gogichaishvili et al. 2014). In overreflection, the amplitude of the reflected wave is higher than the amplitude of the incident wave, i.e., the wave gains energy from the shear flow, or, more correctly, from the source that supports the shear flow. Overreflection is related to a backward nature of the transmitted wave, which changes the sign of the phase velocity due

to the velocity shear, and its energy becomes negative. A wave with negative energy is called a negative energy wave (NEW) (see, e.g., Cairns 1979). The use of this term emphasises that the amplitude of a NEW increases when the energy of the system decreases, for example, due to dissipative and wave leakage processes (e.g., Ostrovskii et al. 1986; Stepanyants & Fabrikant 1989). It leads to the occurrence of various NEW instabilities. Nonlinear coupling of NEWs with regular waves with positive energy can become subject to explosive instabilities which are faster than the standard linear instabilities. MHD waves of negative energy attract attention in the context of the stability of shear flows in natural and laboratory plasmas (e.g., Khalzov et al. 2008; Ilgisonis et al. 2009), including the solar atmosphere (e.g., Joarder et al. 1997; Andries & Goossens 2001; Taroyan & Ruderman 2011; Ballai et al. 2015).

An important feature of NEWs is that they can be unstable for the velocity shear well below the KHI threshold. If the NEW instability is caused by a dissipative process, this phenomenon is called dissipative instability (Cairns 1979; Joarder et al. 1997). Cairns (1979) considered two parallel flows with a perpendicular profile of the velocity in the form of a step function and viscosity in one side, and proposed a criterion for the dissipative instability to occur at a shear flow speed below the KHI threshold. Despite the obvious importance of the effect of NEWs for the plasma non-uniformities of the solar atmosphere, there have been only several dedicated studies of this phenomenon. Adopting Cairns (1979)'s criterion scheme, Joarder et al. (1997) studied the excitation condition for NEWs in a plasma slab, and showed that surface kink modes with negative energy could occur in magnetic structures of the solar photosphere. Ryutova (1988), considering kink modes in the long wavelength limit, was first to show that NEW may be crucial for the energy transfer to the upper solar atmosphere. Ruderman, & Goossens (1995) obtained analytical solutions for the negative energy Alfvén surface wave propagating on a discontinuous shear flow boundary in an incompressible plasma, taking into account viscosity at the one side and a constant flow at the other side. They showed that when the flow speed is above the critical value, one wave mode of two solutions changes the sign of the phase speed, and then two wave modes become co-propagating. The wave mode with the smaller phase speed has negative energy. Its growth rate (increment) increases with the increase in the viscosity coefficient. Recent study by Ruderman (2018) showed that the growth rate of a standing surface wave is equal to the growth rate of the (backward) propagating wave with negative energy minus the damping rate (decre-

ment) of the (forward) propagating wave with positive energy.

In this paper, we investigate the appearance of a negative energy MHD surface mode with an arbitrary azimuthal wave number m in a plasma cylinder penetrated by an axial magnetic field, in the incompressible approximation. We describe the model in Sec. 2, presents the results in Sec. 3, and conclude the paper in Sec. 4

2. MODEL

Our governing equations are the viscous MHD equations for an incompressible plasma:

$$\frac{\partial \rho}{\partial t} + \nabla \cdot (\rho \mathbf{v}) = 0, \quad (1)$$

$$\rho \frac{\partial \mathbf{v}}{\partial t} + \rho \mathbf{v} \cdot \nabla \mathbf{v} + \nabla p - \mathbf{j} \times \mathbf{B} = \eta \nabla^2 \mathbf{v}, \quad (2)$$

$$\frac{\partial p}{\partial t} + \mathbf{v} \cdot \nabla p + \gamma p \nabla \cdot \mathbf{v} = 0, \quad (3)$$

$$\frac{\partial \mathbf{B}}{\partial t} + \nabla \times \mathbf{E} = 0, \quad (4)$$

$$\mathbf{j} - \frac{1}{\mu_0} \nabla \times \mathbf{B} = 0, \quad (5)$$

$$\mathbf{E} + \mathbf{v} \times \mathbf{B} = 0, \quad (6)$$

where \mathbf{v} is the velocity; \mathbf{B} and \mathbf{E} are the magnetic and electric fields, respectively; \mathbf{j} is the electric current density; ρ is the mass density, η is the shear viscosity, μ_0 is the permeability of vacuum, and γ is the ratio of specific heat. We consider an infinitely long, axisymmetric cylindrical magnetic flux tube with radius R , i.e., a plasma cylinder with a sharp boundary, surrounded by a plasma with different physical quantities, similar to the model of Edwin, & Roberts (1983). The magnetic field is parallel to the axis of the cylinder. The equilibrium is reached by the balance of the total pressure inside and outside the cylinder. Inside the cylinder there is a field aligned steady flow, uniform in the radial direction. The external plasma is static. Thus, the boundary of the cylinder is a tangential discontinuity. The plasma outside the cylinder has finite viscosity, while the internal plasma is ideal.

In the following, we linearized Eqs. (1)–(6) in cylindrical coordinates. We consider separately the regions inside and outside the cylinder as homogeneous media. Perturbations are considered to be harmonic in time and with respect to the axial and azimuthal coordinates. Then, applying matching condition at the tube boundary, we derive the dispersion relation and obtain the solutions for the phase speed and damping or growth rate.

2.1. Wave equations

We denote the quantities inside (outside) of the cylinder by a subscript $i(e)$. In the equilibrium, inside the cylinder, the magnetic field is $\mathbf{B}_0 = (0, 0, B_0)$, and the flow is $\mathbf{v}_0 = (0, 0, U_0)$. Both U_0 and B_0 are constants. The plasma density ρ_i is constant too. The Alfvén speed is $v_{Ai} = B_0/\sqrt{\mu_0\rho_i}$. Linearizing the ideal MHD equations with respect to the equilibrium, and applying the Fourier transformation ($\sim \exp[i(k_z z + m\phi - \omega t)$]), we obtain for the perturbations of the radial velocity \hat{v}_{ri} and total pressure \hat{P}_i the following set of coupled ordinary differential equations (see Appendix A),

$$\begin{aligned} -\rho_i(\tilde{\omega}^2 - \omega_{Ai}^2)\hat{v}_{ri} &= i\tilde{\omega}\hat{P}'_i, \\ i\left[\tilde{\omega}^2 - v_{Ai}^2\left(k_z^2 + \frac{m^2}{r^2}\right)\right]\tilde{\omega}\hat{P}_i &= \rho_i v_{Ai}^2(\tilde{\omega}^2 - \omega_{Ai}^2)\frac{(r\hat{v}_{ri})'}{r}, \end{aligned} \quad (7)$$

where $\tilde{\omega} = \omega - k_z U_0$, $\omega_{Ai} = k_z v_{Ai}$, and the prime denotes the derivative with respect to r . Here k_z and m are real, while ω could be complex.

Outside of the cylinder, we assume the same magnetic field as inside it, while the density is ρ_e . Linearization of Eqs. (1)-(6) with the same Fourier transform leads to (see Appendix B)

$$\begin{aligned} \left(L_z^2 + \frac{4m^2\rho_e^2\nu_e^2\omega^2}{r^4}\right)\hat{v}_{re} &= \frac{2m^2\rho_e\nu_e\omega^2}{r^3}\hat{P}_e + i\omega L_z\hat{P}'_e \\ &\quad - \frac{6im\rho_e^2\nu_e^2\omega^2}{r^4}\hat{v}_{\phi e}, \end{aligned} \quad (9)$$

$$\begin{aligned} i\omega\left(L_z + \frac{m^2\rho_e v_{Ae}^2}{r^2}\right)\hat{P}_e &= \rho_e v_{Ae}^2\frac{(r\hat{v}_{re})'}{r} \\ &\quad + \frac{2im^2\rho_e^2\nu_e\omega v_{Ae}^2}{r^3}\hat{v}_{re} \end{aligned} \quad (10)$$

where

$$L_z = -\rho_e\left[\omega^2 - \omega_{Ae}^2 - i\nu_e\omega\left(\mathcal{D} - \frac{1}{r^2}\right)\right], \quad (11)$$

$\nu_e = \eta/\rho_e$, $v_{Ae} = B_0/\sqrt{\mu_0\rho_e}$, and $\mathcal{D}\psi = \frac{(r\psi)'}{r} - \left(\frac{m^2}{r^2} + k_z^2\right)\psi$ for ψ . Notice that \hat{v}_ϕ denotes the perturbation of the azimuthal velocity.

2.2. Dispersion relation

Taking divergence of Eq. (2) yields the condition $\mathcal{D}\hat{P}_{i(e)} = 0$ (see, e.g., Ruderman, & Goossens (1995)), which has Bessel functions as solutions.

In this study we consider surface magnetohydrodynamic modes,

$$\hat{P}_i = A_i I_m(k_z r), \quad (12)$$

$$\hat{P}_e = A_e K_m(k_z r), \quad (13)$$

$$\hat{v}_{ri} = -i\omega\hat{\zeta}_{ri} + ik_z U_0\hat{\zeta}_{ri} = -i\tilde{\omega}\hat{\zeta}_{ri}, \quad (14)$$

$$\hat{v}_{re} = -i\omega\hat{\zeta}_{re}, \quad (15)$$

where A_i and A_e are constant, $I_m(k_z r)$ and $K_m(k_z r)$ are modified Bessel functions of the first and second kinds, respectively, and $\hat{\zeta}_r$ is the Fourier-transformed Lagrangian displacement in the radial direction. Hereafter we use the notations I_m and K_m instead of $I_m(k_z r)$ and $K_m(k_z r)$, respectively.

From the kinematic boundary condition, and continuity condition of the stress tensor at the boundary ($r = R$), we obtain

$$\frac{\partial\hat{v}_z}{\partial r} + ik_z\hat{v}_r = 0, \quad (16)$$

$$\hat{P}_i = \hat{P}_e - 2\rho_e\nu_e\frac{\partial\hat{v}_{re}}{\partial r}, \quad (17)$$

$$\hat{\zeta}_{ri} = \hat{\zeta}_{re}. \quad (18)$$

Next, substituting Eqs. (12)-(17) into Eqs. (7) and (9), we derive

$$\rho_i(\tilde{\omega}^2 - \omega_{Ai}^2)\hat{\zeta}_{ri} = k_z A_i I'_m, \quad (19)$$

$$-i\omega L_z^2\hat{\zeta}_{re} = \frac{2m^2\rho_e\nu_e\omega^2}{r^3}A_e K_m + i\omega k_z A_e L_z K'_m, \quad (20)$$

where the prime denotes the derivative with respect to entire argument $k_z R$. In Eq. (20), we neglect the term with ν_e^2 , assuming the viscosity to be weak, $\nu_e/(\omega R^2) \ll 1$. This condition can be written as $R_e k_z R \gg 1$, where $R_e = \omega R/k_z \nu_e$ is the Reynolds number. For sufficiently large values of R_e , this approximation is valid regardless of the value of $k_z R$ ($R_e \gg k_z R$). In other words, this condition implies that there exists a lower limit (cutoff) to $k_z R$ for a given ν_e such that $k_z R \gg (1/R_e)$, which must be considered for the interpretation of the results in Figs. (7) and (8) in Sec. 3.3.

Then we obtain for A_i and A_e

$$A_i = \frac{\rho_i}{k_z I'_m}(\tilde{\omega}^2 - \omega_{Ai}^2)\hat{\zeta}_{ri}, \quad (21)$$

$$\begin{aligned} A_e &= \frac{\rho_e\left[(\omega^2 - \omega_{Ae}^2) - 2i\nu_e\omega\left(\mathcal{D} - \frac{1}{R^2}\right)\right]\hat{\zeta}_{re}}{k_z K'_m} \\ &\quad \times \left[1 - \frac{i\nu_e\omega\left[\frac{2m^2}{R^3}K_m - k_z\left(\mathcal{D} - \frac{1}{R^2}\right)K'_m\right]}{k_z(\omega^2 - \omega_{Ae}^2)K'_m}\right]. \end{aligned} \quad (22)$$

Combining Eqs. (15) and (17) yields

$$\hat{P}_i = \hat{P}_e + 2i\omega\rho_e\nu_e\frac{\partial\hat{\zeta}_{re}}{\partial r}. \quad (23)$$

Substituting Eqs. (12)-(13) with (21)-(22) into Eq. (23), we obtain

$$\begin{aligned} & \left[\left(\frac{\rho_i I_m}{k_z I'_m} - \frac{\rho_e K_m}{k_z K'_m} \right) \omega^2 - 2k_z U_0 \frac{\rho_i I_m}{k_z I'_m} \omega + \frac{\rho_i I_m}{k_z I'_m} (k_z U_0)^2 - \frac{\rho_i I_m}{k_z I'_m} \omega_{Ai}^2 + \frac{\rho_e K_m}{k_z K'_m} \omega_{Ae}^2 \right] \hat{\zeta}_{ri} \\ & + i\omega \rho_e \nu_e \left\{ \frac{2K_m}{k_z K'_m} \left(\mathcal{D} - \frac{1}{r^2} \right) - \frac{K_m}{k_z K_m'^2} \left[\left(\mathcal{D} - \frac{1}{r^2} \right) K'_m \right] + \frac{2m^2 K_m^2}{k_z^2 R^3 K_m'^2} - 2 \frac{\partial}{\partial r} \right\} \hat{\zeta}_{re} = 0. \end{aligned} \quad (24)$$

As we are interested in the behavior of the wave amplitude in time, we may assume that approximately

$$\hat{\zeta}_{re} \approx \frac{1}{\rho_e (\omega^2 - \omega_{Ae}^2)} \frac{\partial \hat{P}_{re}}{\partial r} = \frac{1}{\rho_e (\omega^2 - \omega_{Ae}^2)} \frac{\partial (A_e K_m)}{\partial r}$$

$$= \frac{k_z A_e K'_m}{\rho_e (\omega^2 - \omega_{Ae}^2)}. \quad (25)$$

Then we obtain the dispersion relation, by using boundary condition (18) and Eq. (25),

$$\begin{aligned} & \left[\left(\frac{\rho_i I_m}{k_z I'_m} - \frac{\rho_e K_m}{k_z K'_m} \right) \omega^2 - 2k_z U_0 \frac{\rho_i I_m}{k_z I'_m} \omega + \frac{\rho_i I_m}{k_z I'_m} (k_z U_0)^2 - \frac{\rho_i I_m}{k_z I'_m} \omega_{Ai}^2 + \frac{\rho_e K_m}{k_z K'_m} \omega_{Ae}^2 \right] \\ & + i\omega \rho_e \nu_e \left[\frac{K_m}{k_z K_m'^2} \left(\mathcal{D} K'_m - \frac{K'_m}{R^2} \right) + \frac{2m^2 K_m^2}{k_z^2 R^3 K_m'^2} - 2k_z \frac{K'_m}{K'_m} \right] = 0. \end{aligned} \quad (26)$$

Equation (26) can be rewritten as

$$D = a\omega^2 + b\omega + c + i d\omega = 0, \quad (27)$$

which is a quadratic equation for ω with the coefficients

$$a = \frac{I_m}{I'_m} - \frac{R_{ei} K_m}{K'_m}, \quad (28)$$

$$b = -2k_z U_0 \frac{I_m}{I'_m}, \quad (29)$$

$$c = k_z^2 v_{Ai}^2 \frac{I_m}{I'_m} \left[\tilde{U}_0^2 - \left(1 - \frac{I'_m K_m}{I_m K'_m} R_{ei} V_{ei}^2 \right) \right], \quad (30)$$

$$d = \nu_e R_{ei} \left[\frac{K_m}{K_m'^2} \left(\mathcal{D} K'_m - \frac{K'_m}{R^2} \right) - 2k_z^2 \frac{K_m''}{K'_m} + \frac{2m^2 K_m^2}{k_z R^3 K_m'^2} \right], \quad (31)$$

and introducing dimensionless ratios $R_{ei} = \rho_e / \rho_i$, $\tilde{U}_0 = U_0 / v_{Ai}$, and $V_{ei} = v_{Ae} / v_{Ai}$. When $U_0 = \eta = 0$, Eq. (27) reduces to the dispersion relation for MHD surface waves in the incompressible limit (Edwin, & Roberts 1983).

Taking that $\omega = \omega_r + i\omega_i$, where ω_r and ω_i are the real and imaginary parts of the cyclic frequency, and assuming $\omega_i \ll \omega_r$, we reduce Eq. (27) to

$$(a\omega_r^2 + b\omega_r + c) + i(2a\omega_r\omega_i + b\omega_i + d\omega_r) = 0. \quad (32)$$

The general analytical solutions for ω_r and ω_i are then

$$\omega_{r\pm} = \frac{-b \pm \sqrt{b^2 - 4ac}}{2a}, \quad (33)$$

$$\omega_{i\pm} = \frac{-d\omega_r}{2a\omega_r + b} = \mp \frac{d\omega_r}{\sqrt{b^2 - 4ac}}. \quad (34)$$

The normalized phase speed \tilde{v}_p and damping (or growth) rate γ are consequently given as

$$\begin{aligned} \tilde{v}_{p\pm} &= \frac{\omega_{r\pm}}{k_z v_{Ai}} \\ &= \frac{\tilde{U}_0 \pm \sqrt{\frac{R_{ei} I'_m K_m}{I_m K'_m} \tilde{U}_0^2 + AB}}{B}, \end{aligned} \quad (35)$$

and

$$\gamma_{\pm} = \frac{\omega_i}{\omega_r} = \quad (36)$$

$$\pm \frac{\tilde{\nu}_e R_{ei} \frac{I'_m}{I_m} \left[\frac{K_m (R^2 \nabla^2 K'_m - K'_m)}{k_z K_m'^2} - 2\tilde{k}_z \frac{K_m''}{K'_m} + \frac{2m^2 K_m^2}{k_z^2 K_m'^2} \right]}{\sqrt{\frac{\rho_{ei} I'_m K_m}{I_m K'_m} \tilde{U}_0^2 + AB}},$$

where $\tilde{\nu}_e = \nu_e / v_{Ai} R$, $\tilde{k}_z = k_z R$, and

$$A = \left(1 - \frac{I'_m K_m}{I_m K'_m} R_{ei} V_{ei}^2 \right), \quad B = \left(1 - \frac{R_{ei} I'_m K_m}{I_m K'_m} \right).$$

The solutions of $c = 0$ and $b^2 - 4ac = 0$ correspond to the critical speed, U_c , and the threshold for KHI, U_{KH} , respectively (e.g., Ruderman, & Goossens 1995):

$$U_c = v_{Ai} \sqrt{1 - \frac{I'_m K_m}{I_m K'_m} R_{ei} V_{ei}^2}, \quad (37)$$

$$U_{KH} = \left[-\frac{I_m K'_m}{R_{ei} I'_m K_m} \left(1 - \frac{R_{ei} I'_m K_m}{I_m K'_m} \right) \right]^{1/2} U_c. \quad (38)$$

We now establish the criterion for the negative energy wave excitation. Using the dispersion relation without viscosity, $D_0 = a\omega^2 + b\omega + c$, we can determine the criterion for the negative wave energy to exist as $C =$

$\omega \frac{\partial D_0}{\partial \omega} < 0$ (Cairns 1979; Joarder et al. 1997). In the absence of the steady flow, we need to have $C > 0$ and find that C is positive except $\omega = 0$. In the presence of flow, from the condition $C < 0$, we obtain the criterion for the occurrence of a negative energy MHD surface wave

$$0 < \omega < \omega_N, \quad \omega_N = -\frac{b}{2a} = \frac{k_z U_0}{1 - \frac{R_{ei} I_m' K_m}{I_m K_m'}}. \quad (39)$$

The condition $\omega (= \omega_r) > 0$ yields the relation $U_0 > U_c$, which is consistent with previous results (e.g., Ruderman, & Goossens 1995).

We point out that if we ignore the term with the factor d in Eq. (32) (no viscosity), Eq. (33) describes the KHI when $b^2 - 4ac < 0$.

3. RESULTS

3.1. Dispersion curves

We first compare the dispersion curves for the phase speed with and without the steady flow. In Fig. 1 we present the phase speed v_p as a function of $k_z R$ for two lowest azimuthal mode numbers and different values of the Alfvén speed ratios V_{ei} in a cylinder with $\tilde{U}_0 = 0$. The phase speed curves obtained in the cases $V_{ei} > 1$ and $V_{ei} < 1$ show different behaviour, which is consistent with the result obtained by Edwin, & Roberts (1983). In the following, we shall denote the higher and lower phase speeds as v_{p+} and v_{p-} , respectively. In the static ($\tilde{U}_0 = 0$) case, the modes with v_{p+} and v_{p-} propagate in the positive and negative z -directions, and $v_{p+} = -v_{p-}$. The dispersion curves for $m > 1$ are similar to $m = 1$ case, but as m increases the curvature of the curves becomes flatter, i.e., the wave dispersion decreases.

Fig. 2 shows the dependence of dispersion curves for $m = 0$ sausage modes on the steady flow speed for two different values of the Alfvén speed ratio V_{ei} . In the presence of the steady flow U_0 , the symmetry of the waves propagating in the opposite directions is broken, i.e., the values of v_{p+} and v_{p-} are affected by the steady flow differently. It is consistent with the result obtained by Joarder et al. (1997). For a sufficiently large U_0 both v_{p+} and v_{p-} are positive. In this regime, the v_{p-} mode becomes a backward wave. For $V_{ei} < 1$, as the steady flow speed U_0 increases, the curve for v_{p+} shifts first upward and then shifts downward, which does not happen for v_{p-} . The curve for v_{p-} goes upward as U_0 increases. On the other hand, for $V_{ei} = 5$, both curves go up with U_0 increment. The same behavior is found for the $m = 1$ kink modes (see Fig. 3). The feature of backward shift for v_{p+} appears to be common for $V_{ei} < 1$, for both $m = 0$ and $m = 1$ modes.

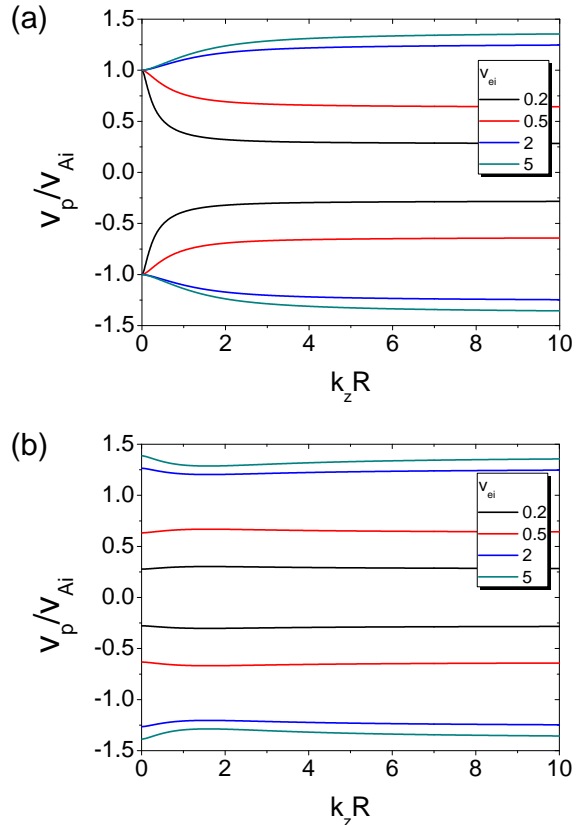


Figure 1. Phase speeds of Alfvén surface modes of an incompressible plasma cylinder as a function of the axial wave number $k_z R$ for (a) $m = 0$ and for (b) $m = 1$ in the case with no steady flow $\tilde{U}_0 = 0$.

3.2. Conditions for the excitation of negative energy waves

From Eq. (39) we infer that in the backward regime, when $v_{p-} > 0$, a mode with v_{p-} can become a NEW. In Fig. 4 we plot several characteristic speeds (v_{p-} , $v_N (= \omega_N / k_z v_{Ai})$, U_c , and U_{KH}), as a function of $k_z R$ for (a) $m = 0$ and (b) $m = 1$, for fixed $\tilde{u}_z (= U_0 / v_{Ai})$ and $V_{ei} < 1$. As inspected in the previous section, it is shown that the condition $U_0 > U_c$ corresponds to $v_{p-} > 0$ and $v_{p-} < v_N$. When \tilde{U}_0 is over 1 for the sausage mode and 1.3 for the kink mode, the backward wave become a NEW, and hence its amplitude can grow exponentially due to one of the NEW instabilities (see Fig. 7 (c)). When U_0 is sufficiently large, the KHI threshold could be reached for certain values of the axial wave number. For the $m = 0$ mode, U_{KH} approaches infinity as $k_z R$ goes to zero, so it is not possible for the sausage surface mode to be KH unstable in the long wavelength limit. Other modes have finite values of U_{KH} .

For $V_{ei} > 1$, the picture slightly changes, see Fig 5. The value of U_{KH} becomes large depending on $R_{ei}(V_{ei})$

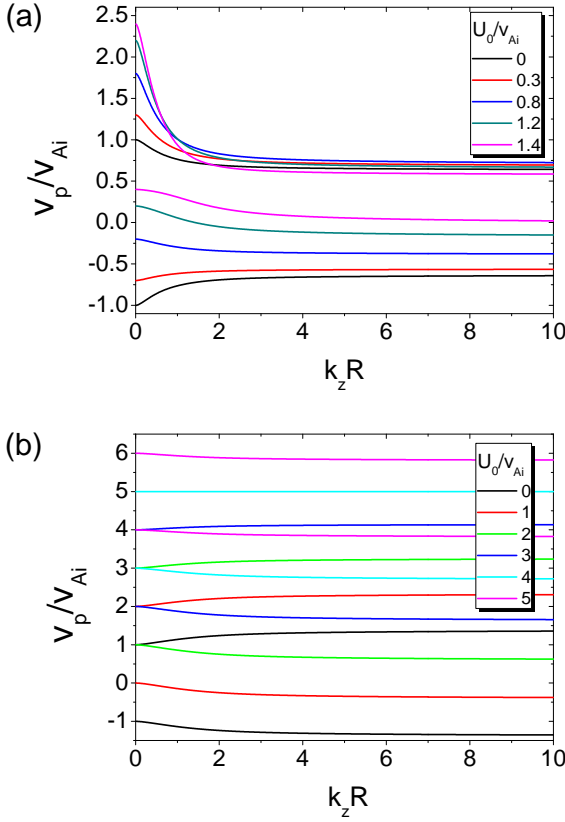


Figure 2. Phase speeds of the sausage mode ($m = 0$) as a function of the axial wave number $k_z R$ for (a) $V_{ei} = 0.5$, and (b) $V_{ei} = 5.0$ for different values of the steady flow speed U_0 .

(see Eq. (38)). The shape of the dependence of v_N also greatly changes. The shape of the U_c curve does not change significantly.

As U_{KH} and U_c both changes with V_{ei} , the interval of the values of U_0 in which NEW instabilities are possible needs to be specified. In Fig. 6, we plot $\Delta U \equiv (U_{KH} - U_c)/v_{Ai}$ versus $k_z R$ for (a) $V_{ei} < 1$ and (b) $V_{ei} > 1$. For positive ΔU , NEW instabilities have lower threshold than KHI. The dependences of ΔU on the axial wave number are different in the cases of $V_{ei} < 1$ and $V_{ei} > 1$. An increase in the Alfvén speed ratio V_{ei} increases the KHI threshold, implying NEW instabilities are more likely.

3.3. Growth rate for the negative energy MHD modes

In the NEW regime, the finite viscosity leads to the amplification of the waves, which is characterised by the imaginary part of the frequency, given by Eq. (36). In Fig. 7 (a), (b), we plot $\gamma_-/\tilde{\nu}_e$, the growth rate γ_- of the backward wave divided by $\tilde{\nu}_e$, versus $k_z R$ for the sausage and kink modes for different shear flow speeds \tilde{U}_0 for both $V_{ei} < 1$ and $\tilde{\nu} = 0.0001$. As \tilde{U}_0 increases,

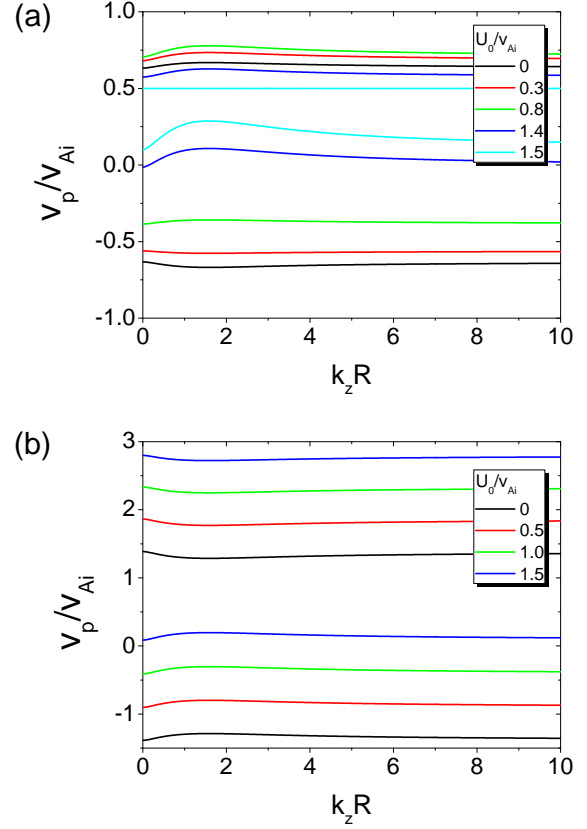


Figure 3. The same as in Fig. 2 but for the kink mode ($m = 1$).

the values of γ_- grows, and its value is higher for the kink mode than for the sausage mode. The growth rate of the kink mode has a minimum near $k_z R = 1$, with its specific value depending on U_0 . In contrast, the growth rate of the sausage mode may have a local maximum, while it keeps growing with the increase in $k_z R$.

In Fig. 7 (c) we show the range of $k_z R$ for the existence of NEW instabilities, which is obtained by applying the condition $U_0 = U_c$. For the sausage mode, the range starts from $k_z R = 0$ where $\tilde{U}_0 = 1$ and extends to larger values of $k_z R$ as \tilde{U}_0 increases. On the other hand, for the kink mode, the NEW unstable range starts from the point $k_z R \approx 1.58$ for the used plasma parameters, and becomes wider with the increase in U_0 . For $m > 0$, it is found that as m increases, γ_- increases in the whole range of $k_z R$. From the results, one may anticipate that the sausage mode is most unstable to NEW instability when $k_z R$ is sufficiently large while higher modes are most unstable in $k_z R \approx 0$. The growth rate for high- m modes becomes large when $k_z R$ approaches zero, which violates the assumption $\omega_i \ll \omega_r$.

The behavior of γ_- for $V_{ei} > 1$ is presented in Fig. 8. The growth rate is much lower than in Fig. 7, implying

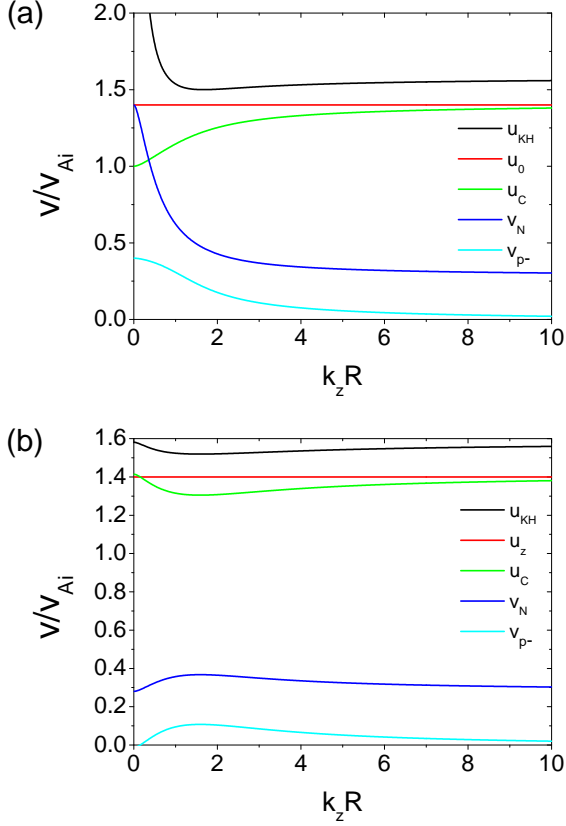


Figure 4. Dependence of the characteristic speeds v_{p^-} , v_N , U_0 , U_{KH} , and U_C on the axial wave number $k_z R$ for (a) $m = 0$ and (b) $m = 1$ modes, for $U_0/v_{Ai} = 1.4$ and $V_{ei} = 0.5$.

that an overdense flux tube is more stable to NEW instabilities than an underdense flux tube. The range of $k_z R$ corresponding to NEW instabilities is the same in both $V_{ei} > 1$ and $V_{ei} < 1$ cases (c).

Eq. (36) shows that γ_{\pm} is proportional to $\tilde{\nu}_e$. Using the estimating expression for the viscosity $\eta \approx 10^{-17} T^{5/2} \text{ kg m}^{-1} \text{ s}^{-1}$ (Hollweg 1986), we have $\tilde{\nu}_e \approx 10^{-17} T^{5/2} / \rho_e v_{Ai} R$ in MKS units. For the typical parameters of a coronal active region, $\rho_e = 0.5 \times 10^{-12} \text{ kg m}^{-3}$, $T = 2.5 \times 10^6 \text{ K}$, $v_{Ai} = 6 \times 10^5 \text{ ms}^{-1}$, and $R = 10^6 \text{ m}$, we obtain $\tilde{\nu}_e \approx 0.33$. Thus, the appearance and growth rate of NEW depend on the background plasma temperature and shear flow speed. The Reynolds number can be written as $Re = (\omega/k_z) / v_{Ai} \tilde{\nu}_e$, from which the valid condition for our approach is induced as $\omega/k_z \gg \tilde{\nu}_e v_{Ai}$. As discussed in Sec. 2.2, it is also necessary to consider the lower limit of $k_z R$ for the valid range of NEW instability for a given ν_e : $k_z R \gg (1/Re)$.

4. CONCLUSIONS AND DISCUSSIONS

We studied conditions for the existence of NEW surface MHD waves in a cylindrical flux tube with a shear

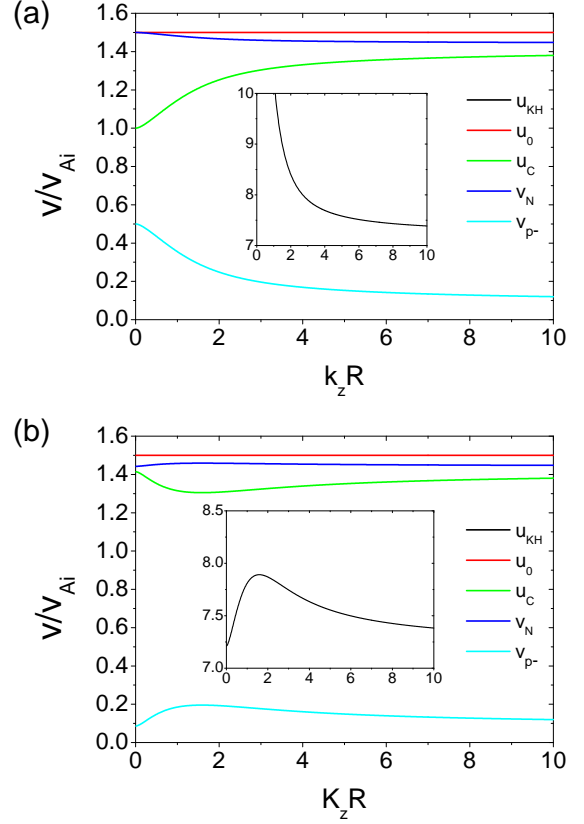


Figure 5. The same as in Fig. 4, but for $U_0/v_{Ai} = 1.5$ and $V_{ei} = 5$

flow in the incompressible limit. The equilibrium plasma density and shear flow experience a sharp change at the boundary of the tube. By matching the boundary condition at the tube boundary, we derived analytically dispersion relations for Alfvénic perturbations, and analysed dependences of the phase speed and growth rate on the plasma parameters. Instabilities associated NEW can be excited when the shear flow speed is between the critical speed for the appearance of NEW, U_C and the KHI threshold, U_{KH} . In other words, the steady flow shear which leads to the occurrence of NEW instabilities could be significantly lower than the KHI threshold. For example, in the long wavelength regime, the NEW instability threshold requires the flow speed shear several times lower than the KHI threshold. A similar result was obtained for the kink mode by Ryutova (1988) in the thin flux tube approximation. Moreover, the critical value of the flow shear for the onset of NEW instabilities should be comparable, only 20%–40% higher than the Alfvén speed inside the plasma cylinder. Such flow shears could be reached in various solar coronal plasma jets (see, e.g. Raouafi et al. 2016), making them subject to NEW instabilities. Thus, NEW effects could be

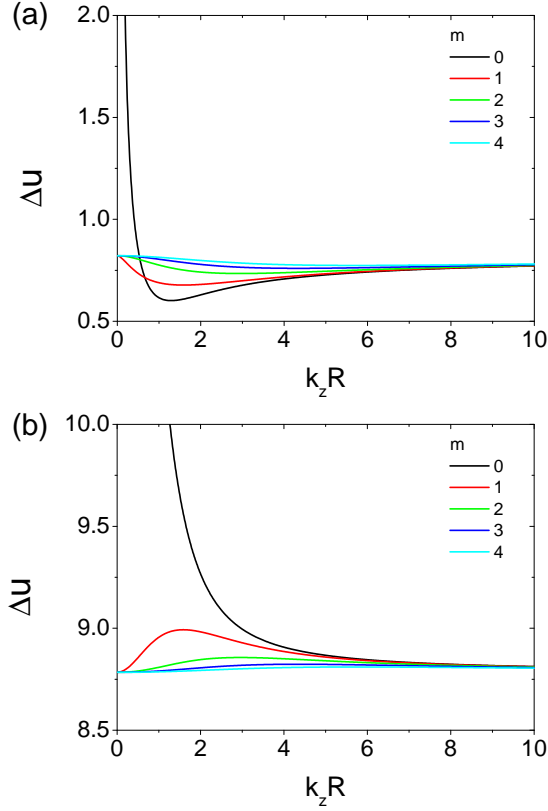


Figure 6. The difference between the thresholds of KHI and NEW instabilities $\Delta U (= (U_{KH} - U_c)/v_{Ai})$ vs the axial wave number $k_z R$ for (a) $V_{ei} = 0.5$ and (b) $V_{ei} = 5$.

responsible for the occurrence of kink oscillations on a hot plasma jet, analysed by [Vasheghani Farahani et al. \(2009\)](#).

For the shear flow speeds lower than the KHI threshold, NEW are found to appear for all axial wave numbers. More rigorously, the shear flow range that corresponds to NEW phenomena, $U_c < U_0 < U_{KH}$, is found to depend on the Alfvén speed contrast inside and outside the flux tube, and also on the axial wave number of the perturbation. For all considered combinations of the parameters, the threshold value of the shear flow for the appearance of sausage NEW is lowest for the longest axial wavelengths, while the minimum value of the shear flow for kink waves is reached for the axial wavelength comparable to the diameter of the cylinder. This allows for the excitation of quasi-monochromatic perturbations by a NEW instability at a coronal jet, which is consistent with the findings of [Vasheghani Farahani et al. \(2009\)](#). It is easier to excite MHD NEW in an underdense flux tube than in an overdense one, which may be used in the interpretation of kink waves observed in supra-arcade flows ([Verwichte et al. 2005](#); [Costa et al. 2009](#)). It may

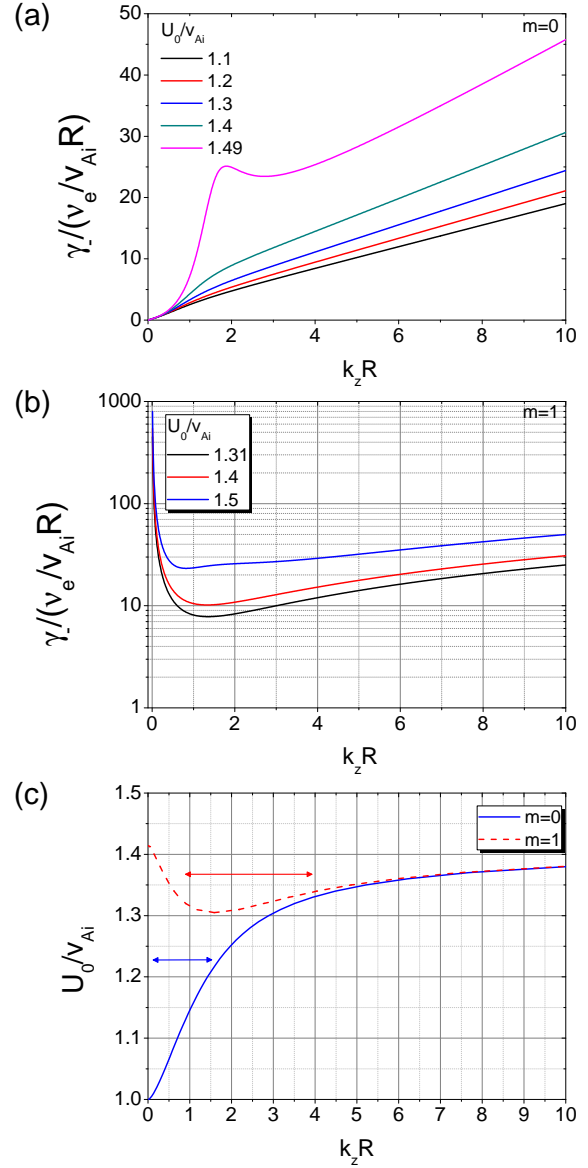


Figure 7. The curve of $\gamma_i/\tilde{\nu}_e$ vs $k_z R$ for (a) $m = 0$ and (b) $m = 1$ modes, and (c) the range of $k_z R$ (denoted by the arrows) for the existence of NEW instabilities for $V_{ei} = 0.5$ and $\tilde{\nu}_e = 0.0001$.

also play an important role in the MHD wave generation and propagation in other plasma non-uniformities with field-aligned shear flows in the solar atmosphere, in particular, in the photosphere and chromosphere.

As an example of a NEW instability, we demonstrated the occurrence of dissipative NEW instability caused by finite viscosity, and found that the instability increment depends strongly on the plasma temperature and the shear flow speed. The excitation of non-axisymmetric NEW, i.e., with $m > 0$, such as kink waves, is most effective in the long wavelength limit. Our results indicate

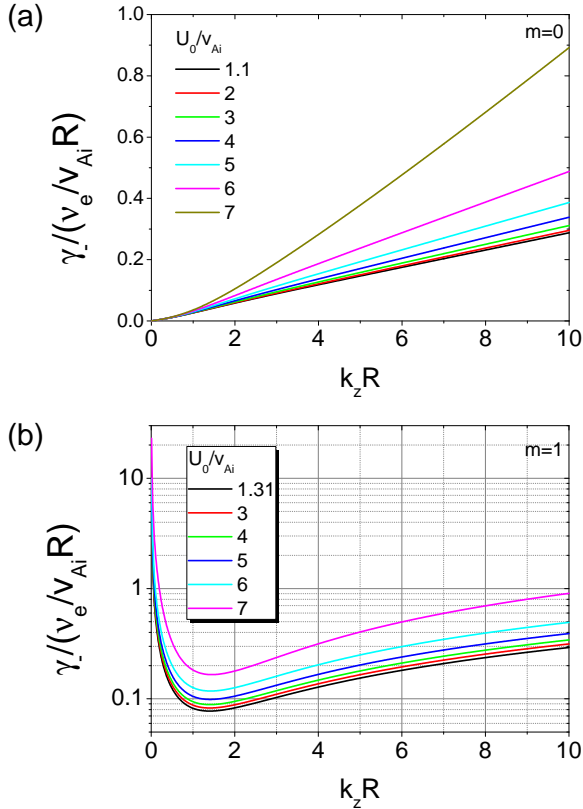


Figure 8. The same as in Fig. 7 (a) and (b), but for $V_{ei} = 5$. The range of $k_z R$ for the excitation condition of NEW instabilities is the same as Fig. 7 (c).

that the omnipresence of inhomogeneous flows in the Sun’s atmosphere (e.g., Morgan, & Hutton 2018) may lead to the effective excitation of guided MHD waves by NEW instabilities. In particular, the NEW effect may be responsible for decayless (undamped) kink oscillations (see, e.g., Nakariakov et al. 2016), which would require a dedicated study in the compressible regime typical for the solar corona. In addition, the developed model may have applications to the solar wind, the Earth’s magnetotail and other plasma environments with shear flows.

Our results are based on the assumption that the viscosity, which is assumed small, only affects the temporal behavior of the wave displacement, which may be valid in the early stage of the NEW instability. Our theory can be tested and its valid range can be investigated rigorously in the numerical simulations.

ACKNOWLEDGMENTS

The authors are grateful to the anonymous referee for his/her crucial and invaluable comments which led to a significant improvement of the manuscript. D.J.Y. and V.M.N. acknowledge the support by the BK21 plus program through the National Research Foundation (NRF) funded by the Ministry of Education of Korea. V.M.N. acknowledges the Russian Foundation for Basic Research Grant No. 18-29-21016.

APPENDIX

A. WAVE EQUATION INSIDE THE FLUX TUBE

Inside the flux tube, using Eqs. (1)-(6), and assuming an axial constant magnetic field $\mathbf{B}_0 = (0, 0, B_0)$ and a background steady flow U_0 along the field, the perturbed quantities of the radial and azimuthal velocities, magnetic field components, and total pressure, v_r , v_ϕ , b_r , b_ϕ , b_z , and $P (= B_0 b_z / \mu_0)$, can be written as

$$\rho_i \mathcal{F}_u v_{ri} = -P'_i + \frac{\mathcal{F}_B}{\mu_0} b_{ri}, \quad (\text{A1})$$

$$\rho_i \mathcal{F}_u v_{\phi i} = \frac{\mathcal{F}_B}{\mu_0} b_{\phi i} - \frac{1}{r} \frac{\partial P_i}{\partial \phi}, \quad (\text{A2})$$

$$\mathcal{F}_u b_{ri} = \mathcal{F}_B v_{ri}, \quad (\text{A3})$$

$$\mathcal{F}_u b_{\phi i} = \mathcal{F}_B v_{\phi i}, \quad (\text{A4})$$

$$\begin{aligned} \dot{b}_{zi} = & -\frac{B_0(rv_{ri})'}{r} - \frac{B_0}{r} \frac{\partial v_{\phi i}}{\partial \phi} \\ & + \frac{(rU_0 b_{ri})'}{r} + \frac{U_0}{r} \frac{\partial b_{\phi i}}{\partial \phi}, \end{aligned} \quad (\text{A5})$$

where prime and dot denote the derivative with respect to r and time, respectively, and

$$\mathcal{F}_u = \frac{\partial}{\partial t} + U_0 \frac{\partial}{\partial z}, \quad \mathcal{F}_B = B_0 \frac{\partial}{\partial z}. \quad (\text{A6})$$

From Eq. (A5), we obtain the equation for P

$$\begin{aligned} \mathcal{F}_u \dot{P}_i = & -\frac{B_0(rB_0)'}{\mu_0 r} \mathcal{F}_u v_{ri} - \frac{B_0^2}{\mu_0} \mathcal{F}_u v'_{ri} - \frac{B_0^2}{\mu_0 r} \frac{\partial \dot{v}_{\phi i}}{\partial \phi} \\ & + \frac{B_0}{\mu_0 r} \mathcal{F}_u (rU_0 b_{ri})'. \end{aligned} \quad (\text{A7})$$

With Eqs. (A2)-(A3) and (A7), by applying \mathcal{F}_u to Eqs. (A1) and (A7), we derive the wave equations for P and v_r ,

$$\mathcal{L}_z v_{ri} = -\mathcal{F}_u P'_i, \quad (\text{A8})$$

$$\left(\mathcal{L}_z - \frac{\rho_i v_{Ai}^2}{r^2} \frac{\partial^2}{\partial \phi^2} \right) \dot{P}_i = \quad (\text{A9})$$

$$\mathcal{L}_z \left[-\frac{B_0^2}{\mu_0 r} v_{ri} - \frac{B_0^2}{\mu_0} v'_{ri} + \frac{B_0}{\mu_0 r} (rU_0 b_{ri})' \right],$$

where

$$\mathcal{L}_z = \rho_i \mathcal{F}_u^2 - \frac{B_0^2}{\mu_0} \frac{\partial^2}{\partial z^2}. \quad (\text{A10})$$

B. WAVE EQUATION OUTSIDE THE FLUX TUBE

With the same axial magnetic field B_0 as inside the flux tube, assuming shear viscosity and no background flow, and using Eqs. (1)-(6), we obtain for v_r , v_ϕ , b_r , and P ,

$$\rho_e F_a v_{re} = -\frac{2\rho_e \nu_e}{r^2} \frac{\partial v_{\phi e}}{\partial \phi} - P'_e + \frac{\mathcal{F}_B}{\mu_0} b_{re}, \quad (\text{B11})$$

$$\rho_e F_a v_{\phi e} = \frac{2\rho_e \nu_e}{r^2} \frac{\partial v_{re}}{\partial \phi} - \frac{1}{r} \frac{\partial P_e}{\partial \phi} + \frac{\mathcal{F}_B}{\mu_0} b_{\phi e}, \quad (\text{B12})$$

$$\dot{b}_{re} = \mathcal{F}_B v_{re}, \quad (\text{B13})$$

$$\dot{b}_{\phi e} = \mathcal{F}_B v_{\phi e}, \quad (\text{B14})$$

$$\dot{b}_{ze} = -\frac{B_0(rv_{re})'}{r} - \frac{B_0}{r} \frac{\partial v_{\phi e}}{\partial \phi}, \quad (\text{B15})$$

where $\nu_e = \mu / \rho_e$ and

$$F_a = \frac{\partial}{\partial t} - \nu_e \left(\mathcal{D} - \frac{1}{r^2} \right). \quad (\text{B16})$$

From Eq. (B15) we obtain the equation for P

$$\dot{P}_e = K_a v_{re} + K_b v'_{re} + K_c v_{\phi e}, \quad (\text{B17})$$

where

$$K_a = -\frac{B_0^2}{\mu_0 r}, \quad K_b = -\frac{B_0^2}{\mu_0}, \quad K_c = -\frac{B_0^2}{\mu_0 r} \frac{\partial}{\partial \phi}. \quad (\text{B18})$$

Taking time derivative of Eqs. (B11)-(B12) results in

$$\rho_e F_a \dot{v}_{re} = J_a v_{re} + J_c v_{\phi e} - \dot{P}'_e, \quad (\text{B19})$$

$$L_z v_{\phi e} = L_{a1} v_r + L_{d1} \dot{P}_e, \quad (\text{B20})$$

where

$$J_a = \frac{B_0^2}{\mu_0} \frac{\partial^2}{\partial z^2}, \quad J_c = -\frac{2\rho_e \nu_e}{r^2} \frac{\partial^2}{\partial \phi \partial t},$$

$$L_z = \rho_e F_a \frac{\partial}{\partial t} - \frac{B_0^2}{\mu_0} \frac{\partial^2}{\partial z^2},$$

$$L_{a1} = \frac{2\rho_e \nu_e}{r^2} \frac{\partial^2}{\partial \phi \partial t}, \quad L_{d1} = -\frac{1}{r} \frac{\partial}{\partial \phi}. \quad (\text{B21})$$

With Eq. (B20), by applying L_z to Eqs. (B17) and (B19), we derive the equations for v_r and P

$$\begin{aligned} \rho_e L_z F_a \dot{v}_{re} = & L_z J_a v_{re} + \left(J_c L_z + \frac{6\rho_e^2 \nu^2}{r^4} \frac{\partial^3}{\partial \phi \partial t^2} \right) v_{\phi e} \\ & - L_z \dot{P}'_e, \end{aligned} \quad (\text{B22})$$

$$(L_z - K_c L_{d1}) \dot{P}_e = (L_z K_a + K_c L_{a1}) v_{re} + K_b L_z v'_{re}. \quad (\text{B23})$$

REFERENCES

- Andries, J., & Goossens, M. 2001, *A&A*, 368, 1083
- Anfinogentov, S. A., Nakariakov, V. M., & Nisticò, G. 2015, *A&A*, 583, A136
- Ballai, I., Oliver, R., & Alexandrou, M. 2015, *A&A*, 577, A82
- Cairns, R. A. 1979, *Journal of Fluid Mechanics*, 92, 1
- Chandrasekhar, S. 1961, *Hydrodynamic and Hydromagnetic Stability*
- Costa, A., Elaskar, S., Fernández, C. A., et al. 2009, *MNRAS*, 400, L85
- De Moortel, I., & Nakariakov, V. M. 2012, *Philosophical Transactions of the Royal Society of London Series A*, 370, 3193
- Edwin, P. M., & Roberts, B. 1983, *SoPh*, 88, 179
- Fejer, J. A. 1963, *Physics of Fluids*, 6, 508
- Gogichaishvili, D., Chagelishvili, G., Chanishvili, R., et al. 2014, *Journal of Plasma Physics*, 80, 667
- Goossens, M., Hollweg, J. V., & Sakurai, T. 1992, *SoPh*, 138, 233
- Goossens, M. L., Arregui, I., & Van Doorselaere, T. 2019, *Frontiers in Astronomy and Space Sciences*, 6, 20
- Hindman, B. W., & Jain, R. 2015, *ApJ*, 814, 105
- Hollweg, J. V. 1986, *ApJ*, 306, 730
- Ilgisonis, V. I., Khalzov, I. V., & Smolyakov, A. I. 2009, *Nuclear Fusion*, 49, 035008
- Jess, D. B., & Verth, G. 2016, *Washington DC American Geophysical Union Geophysical Monograph Series*, 216, 449
- Joarder, P. S., Nakariakov, V. M., & Roberts, B. 1997, *SoPh*, 176, 285
- Khalzov, I. V., Smolyakov, A. I., & Ilgisonis, V. I. 2008, *Physics of Plasmas*, 15, 054501
- Luna, M., Terradas, J., Oliver, R., et al. 2009, *ApJ*, 692, 1582
- McKenzie, J. F. 1970, *Planet. Space Sci.*, 18, 1
- Morgan, H., & Hutton, J. 2018, *ApJ*, 853, 145
- Nakariakov, V. M., & Roberts, B. 1995, *SoPh*, 159, 213
- Nakariakov, V. M., Anfinogentov, S. A., Nisticò, G., et al. 2016, *A&A*, 591, L5
- Nakaryakov, V. M., & Stepanyants, Y. A. 1994, *Astronomy Letters*, 20, 763
- Ostrovskii, L. A., Rybak, S. A., & Tsimring, L. S. 1986, *Soviet Physics Uspekhi*, 29, 1040
- Raouafi, N. E., Patsourakos, S., Pariat, E., et al. 2016, *SSRv*, 201, 1
- Ruderman, M. S., & Goossens, M. 1995, *Journal of Plasma Physics*, 54, 149
- Ruderman, M. S. 2018, *Journal of Plasma Physics*, 84, 905840101
- Ruderman, M. S., & Roberts, B. 2002, *ApJ*, 577, 475
- Ryutova, M. P. 1988, *Soviet Journal of Experimental and Theoretical Physics*, 67, 1594
- Sen, A. K. 1963, *Physics of Fluids*, 6, 1154
- Stepanyants, Y. A., & Fabrikant, A. L. 1989, *Soviet Physics Uspekhi*, 32, 783
- Taroyan, Y., & Ruderman, M. S. 2011, *SSRv*, 158, 505
- Van Doorselaere, T., Ruderman, M. S., & Robertson, D. 2008, *A&A*, 485, 849
- Vasheghani Farahani, S., Van Doorselaere, T., Verwichte, E., et al. 2009, *A&A*, 498, L29
- Verth, G., & Jess, D. B. 2016, *Washington DC American Geophysical Union Geophysical Monograph Series*, 216, 431
- Verwichte, E., Nakariakov, V. M., & Cooper, F. C. 2005, *A&A*, 430, L65
- Zaqarashvili, T. V., Zhelyazkov, I., & Ofman, L. 2015, *ApJ*, 813, 123